

Very early warning of next El Niño

Josef Ludescher^a, Avi Gozolchiani^b, Mikhail I. Bogachev^{a,c}, Armin Bunde^a, Shlomo Havlin^b, and Hans Joachim Schellnhuber^{d,e,1}

^aInstitut für Theoretische Physik, Justus-Liebig-Universität Giessen, D-35392 Giessen, Germany; ^bDepartment of Physics, Bar-Illan University, Ramat Gan 52900, Israel; ^cRadio Systems Department, St. Petersburg Electrotechnical University, St. Petersburg 197376, Russia; ^dPotsdam Institute for Climate Impact Research, 14412 Potsdam, Germany; and ^eSanta Fe Institute, Santa Fe, NM 87501

Edited by W. G. Ernst, Stanford University, Stanford, CA, and approved January 9, 2014 (received for review December 6, 2013)

The most important driver of climate variability is the El Niño Southern Oscillation, which can trigger disasters in various parts of the globe. Despite its importance, conventional forecasting is still limited to 6 mo ahead. Recently, we developed an approach based on network analysis, which allows projection of an El Niño event about 1 y ahead. Here we show that our method correctly predicted the absence of El Niño events in 2012 and 2013 and now announce that our approach indicated (in September 2013 already) the return of El Niño in late 2014 with a 3-in-4 likelihood. We also discuss the relevance of the next El Niño to the question of global warming and the present hiatus in the global mean surface temperature.

dynamic networks | ENSO | spring barrier

El Niño Southern Oscillation

Natural climate variability is driven by numerous processes, but the most important one is the El Niño-Southern Oscillation (ENSO) phenomenon (1–5). It can be perceived as a self-organized dynamical see-saw pattern in the Pacific ocean-atmosphere system, featured by rather irregular warm (El Niño) and cold (La Niña) excursions from the long-term mean state. The ENSO phenomenon is tracked and quantified by the NINO3.4 index, which is defined as the

average of the sea surface temperature (SST) anomalies at certain grid points in the Pacific (Fig. 1). An El Niño episode is said to occur when the index is 0.5 °C above the average for a period of at least 5 mo.

Because especially strong El Niño episodes can wreak havoc in various parts of the world (through extreme weather events and other environmental perturbations) (6–10), early warning schemes based on robust scientific evidence are highly desirable. Sophisticated global climate models taking into account the

atmosphere-ocean coupling, as well as statistical approaches like the dynamical systems schemes approach, autoregressive models, and pattern recognition techniques, have been used to forecast the pertinent index with lead times between 1 and 24 mo (1, 11–26). Monthly updated overviews of the current conventional forecasts can be obtained from the International Research Institute for Climate and Society (27) and the National Oceanic and Atmospheric Administration (28). Unfortunately, the forecasting methods used thus far have quite limited anticipation power. In particular, they generally fail to overcome the so-called “spring barrier” (29, 30), which shortens their warning time to around 6 mo.

To resolve this problem, we recently introduced an alternative forecasting approach (31) based on complex networks analysis (32–35) that can considerably shift the probabilistic prediction horizon. The approach exploits the remarkable observation that a large-scale cooperative mode linking the “El Niño basin” (i.e., the equatorial Pacific corridor) and the rest of the Pacific ocean (Fig. 1) builds up in the calendar year before a pronounced El Niño event. An appropriate measure for the emerging cooperativity can be derived from the time evolution of the teleconnections (links) between the atmospheric temperatures at the grid points (nodes) inside and outside of the El Niño basin. The strengths of those links are represented by the

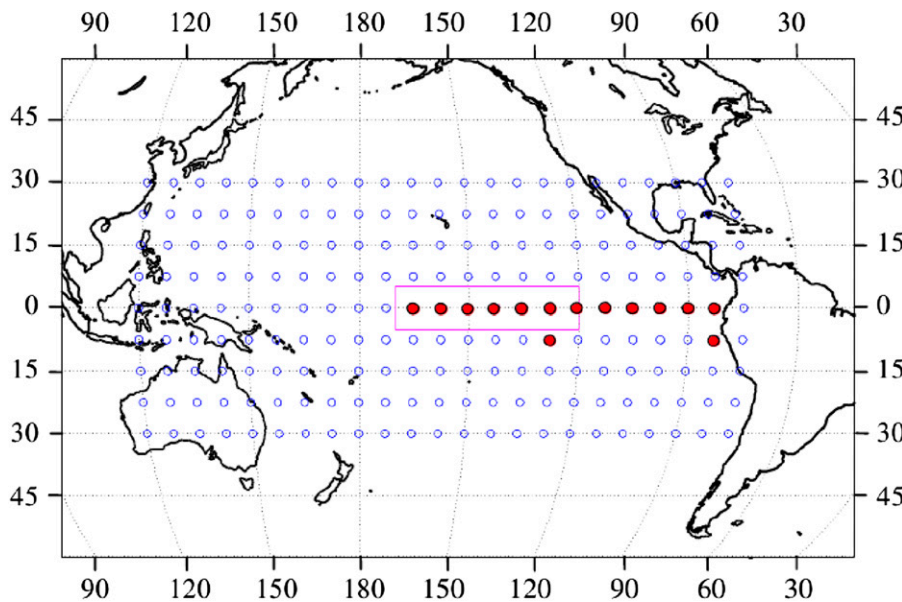


Fig. 1. The NINO3.4 index and the climate network. The network consists of 14 grid points in the El Niño basin (solid red symbols) and 193 grid points outside this domain (open symbols). The red rectangle denotes the area where the NINO3.4 index is measured. The grid points are considered as the nodes of the climate network that we use here to forecast El Niño events. Each node inside the El Niño basin is linked to each node outside the basin. The nodes are characterized by their surface air temperature (SAT), and the link strength between the nodes is determined from their cross-correlation (see below). The figure is from ref. 31.

Author contributions: J.L., A.G., M.I.B., A.B., S.H., and H.J.S. wrote the paper.

The authors declare no conflict of interest.

This article is a PNAS Direct Submission.

¹To whom correspondence should be addressed. E-mail: john@pik-potsdam.de.

values of the respective cross-correlations (*Data and Methods*). The crucial entity is the mean link strength $S(t)$ as obtained by averaging over all individual links in the network at a given instant t (for details, see refs. 31 and 35 and *Data and Methods*). $S(t)$ rises when the cooperative mode builds up and drops again when this mode collapses rather conspicuously with the onset of the El Niño event. The rise of $S(t)$ in the year before an El Niño event starts serves as a precursor for the event.

Forecasting the Next El Niño

For the sake of concrete forecasting, we used in ref. 31 high-quality atmospheric temperature data for the 1950–2011 period. The optimized algorithm (*Data and Methods*) involves an empirical decision threshold Θ . Whenever S crosses Θ from below while the system is outside the El Niño mode, the algorithm sounds an alarm and predicts El Niño inception in the following year. For obtaining and testing the appropriate thresholds, we divided the data into two halves. In the first part (1950–1980), which represents the learning phase, all thresholds above the temporal mean of $S(t)$ are considered, and the optimal ones, i.e., those ones that lead to the best predictions in the learning phase, are determined. We found that Θ -values between 2.815 and 2.834 lead to the best performance (31). In the second part of the data set (1981–2011), which represents the prediction (hindcasting) phase, the performance of these thresholds was tested. We found that the thresholds between 2.815 and 2.826 gave the best results (Fig. 2, where $\Theta = 2.82$). The alarms were correct in 76% and the nonalarms in 86% of all cases.

For Θ values between 2.827 and 2.834, the performance was only slightly weaker.

Now, equipped with this hindcasting capacity of the algorithm, we turn to present and future El Niño behavior by considering all available temperature data, which extends the prediction phase from the end of 2011 until November 2013. Fig. 2A shows that in 2011 and 2012, $S(t)$ did not cross the threshold from below, which correctly forecasted the absence of El Niño events in both 2012 and 2013. These predictions, made by the end of 2011 and 2012, respectively, are not trivial. For example, as late as August 2012, the Climate Prediction Center/International Research Institute for Climate and Society Consensus Probabilistic ENSO forecast focusing on the SSTs in the NINO3.4 domain yielded a 4-in-5 likelihood for an El Niño event in 2012, which turned out to be incorrect only few months later (27, 28).

However, as Fig. 2B reveals, a sea change seems to be underway now. Between September 7 (where $S = 2.810$ and was below the lowest threshold of 2.815) and September 17 (where $S = 2.838$ was above the upper thresholds of 2.826 and 2.834), $S(t)$ transgressed the alarm threshold band, indicating the return of El Niño in 2014.

Thus, our scheme generates an early warning signal with a 3-in-4 likelihood. Note that conventional forecasting methods focusing on SSTs in the NINO 3.4 domain (27, 28) keep predicting ENSO-neutral conditions. In September 2013, the CPC/IRI consensus probabilistic ENSO forecast yielded a 1-in-5 likelihood for an ENSO event next year, which increased to a 1-in-3 likelihood by November 2013. We are aware of the reputational risks associated with our

announcement, yet formulating falsifiable hypotheses is at the heart of the scientific method. Should our alarm turn out to be correct, however, this would be a major step toward better forecasting—and eventually understanding—of the ENSO dynamics.

Our contribution may also be relevant for the wider debate about anthropogenic global warming (36). There have been speculations that the recent hiatus in planetary mean surface temperature rise indicates that the climate system is less CO₂ sensitive than previously thought. On the other hand, new studies have demonstrated that decadal atmospheric warming is considerably masked by equatorial Pacific variability in heat uptake and release (36–39).

In fact, an average El Niño event increases the climate anomaly (deviation of global mean surface temperature from preindustrial level) by about 0.1 °C. The mean anomaly in the La Niña-dominated period 2002–2011 was 0.59 °C, whereas the record temperature deviation thus far happened in 2010 (0.69 °C) (40). This suggests that a strong El Niño event in late 2014 (as indicated by our scheme) can make 2015 a record year, because air temperature rise lags Pacific warming by about 3 mo.

On the other hand, the signal depicted in Fig. 2B is relatively weak thus far. However, we have not yet explored how the strength of the precursor cooperativity pattern relates to the degree of the ensuing Eastern Pacific warming. This is an important topic for future research.

Data and Methods

For the prediction of El Niño events or nonevents, we use the cooperative behavior of the atmospheric temperatures in the Pacific as precursor. To obtain a measure for the cooperativity, we consider the daily surface atmospheric temperatures (SATs) between June 1948 and November 2013 at grid points (nodes) of a Pacific network (Fig. 1).

We analyze the time evolution of the teleconnections (links) between the temperatures at nodes i inside the El Niño basin and nodes j outside the basin. The strengths of these links are represented by the strengths of the cross-correlations between the temperature records at these sites (35).

The prediction algorithm (31) is as follows:

- i) At each node k of the network shown in Fig. 1, the daily atmospheric temperature anomalies $T_k(t)$ (actual temperature value minus climatological average for each calendar day; see below) at the surface area level are determined. For the calculation of the climatological average, leap days were removed. The data were obtained from the

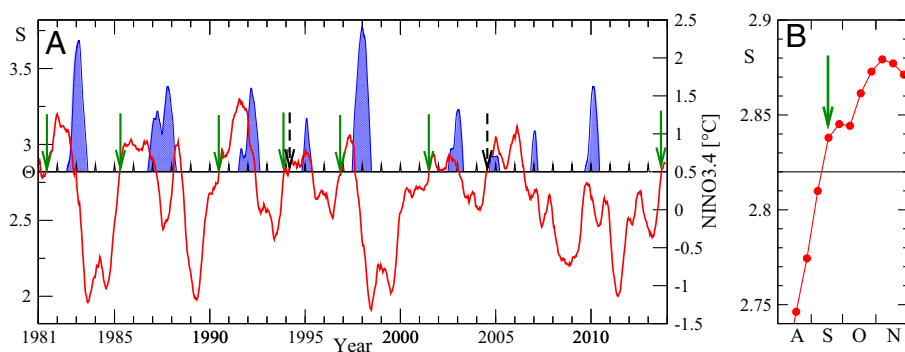


Fig. 2. The forecasting scheme. (A) We compare the average link strength $S(t)$ in the climate network (red curve) with a decision threshold Θ (horizontal line, here $\Theta = 2.82$; left scale) and the standard NINO3.4 index (right scale) between January 1981 and November 2013. When the link strength crosses the threshold from below, outside an El Niño episode, we give an alarm and predict that an El Niño episode will start in the following calendar year. The El Niño episodes (when the NINO3.4 index is above 0.5 °C for at least 5 mo) are shown by the solid blue areas. Correct predictions are marked by green arrows and false alarms by dashed arrows. (B) Magnification of A for August (A), September (S), October (O), and November (N) 2013. The figure shows that by September 17 (green arrow), the optimal decision thresholds have been crossed, forecasting an El Niño event in 2014. In A, the learning phase (1950–1980) where the optimal thresholds have been learned has been omitted (31).

National Centers for Environmental Prediction/National Center for Atmospheric Research Reanalysis I project (41, 42).

ii) For obtaining the time evolution of the strengths of the links between the nodes i inside the El Niño basin and the nodes j outside, we compute, for each 10th day t in the considered time span between January 1950 and November 2013, the time-delayed cross-correlation function defined as

$$C_{ij}^{(t)}(-\tau) = \frac{\langle T_i(t)T_j(t-\tau) \rangle - \langle T_i(t) \rangle \langle T_j(t-\tau) \rangle}{\sqrt{\langle (T_i(t) - \langle T_i(t) \rangle)^2 \rangle} \cdot \sqrt{\langle (T_j(t-\tau) - \langle T_j(t-\tau) \rangle)^2 \rangle}}, \quad [1]$$

and

$$C_{ij}^{(t)}(\tau) = \frac{\langle T_i(t-\tau)T_j(t) \rangle - \langle T_i(t-\tau) \rangle \langle T_j(t) \rangle}{\sqrt{\langle (T_i(t-\tau) - \langle T_i(t-\tau) \rangle)^2 \rangle} \cdot \sqrt{\langle (T_j(t) - \langle T_j(t) \rangle)^2 \rangle}}, \quad [2]$$

where the brackets denote an average over the last 365 d, according to

$$\langle f(t) \rangle = \frac{1}{365} \sum_{m=0}^{364} f(t-m). \quad [3]$$

We consider time lags τ between 0 and 200 d, where a reliable estimate of the background noise level can be guaranteed.

iii) We determine, for each point in time t , the maximum, the mean, and the SD around the mean of the absolute value of the cross-correlation function $|C_{ij}^{(t)}(\tau)|$ and define the link strength $S_{ij}(t)$ as the difference

between the maximum and the mean value, divided by the SD. Accordingly, S_{ij} describes

the link strength at day t relative to the underlying background noise (signal-to-noise ratio) and thus quantifies the dynamical teleconnections between nodes i and j .

iv) To obtain the desired mean strength $S(t)$ of the dynamical teleconnections in the climate network, we simply average over all individual link strengths.

v) Finally, we compare $S(t)$ with decision thresholds Θ . When the link strength $S(t)$ (being above its temporal mean) crosses the threshold from below and the NINO3.4 index is below 0.5°C , we give an alarm and predict that an El Niño episode will start in the following calendar year.

We would like to add that, for the calculation of the climatological average in the learning phase, all data within this time window were taken into account, whereas in the prediction phase, only data from the past up to the prediction date were considered.

ACKNOWLEDGMENTS. A.B. and S.H. thank Deutsche Forschungsgemeinschaft for financial support. S.H. also acknowledges financial support by the Learning about Interacting Networks in Climate project funded by the Marie-Curie Initial Training Networks program (FP7-PEOPLE-2011-ITN).

- 1 Clarke AJ (2008) *An Introduction to the Dynamics of El Niño the Southern Oscillation* (Elsevier Academic Press, London).
- 2 Sarachik ES, Cane MA (2010) *The El Niño-Southern Oscillation Phenomenon* (Cambridge Univ Press, Cambridge, UK).
- 3 Power S, Delage F, Chung C, Kociuba G, Keay K (2013) Robust twenty-first-century projections of El Niño and related precipitation variability. *Nature* 502(7472):541–545.
- 4 Dijkstra HA (2005) *Nonlinear Physical Oceanography: A Dynamical Systems Approach to the Large-Scale Ocean Circulation and El Niño* (Springer, New York).
- 5 Wang C, et al. (2012) El Niño and Southern Oscillation (ENSO): A review. *Coral Reefs of the Eastern Pacific* (Springer, Berlin), pp 3–19.
- 6 Wen C (2002) Impacts of El Niño and La Niña on the cycle of the East Asian winter and summer monsoon. *Chin J Atmos Sci* 5:595–610.
- 7 Corral A, Ossó A, Llebort JE (2010) Scaling of tropical-cyclone dissipation. *Nat Phys* 6(9):693–696.
- 8 Donnelly JP, Woodruff JD (2007) Intense hurricane activity over the past 5,000 years controlled by El Niño and the West African monsoon. *Nature* 447(7143):465–468.
- 9 Kovats RS, Bouma MJ, Hajat S, Worrall E, Haines A (2003) El Niño and health. *Lancet* 362(9394):1481–1489.
- 10 Davis M (2001) *Late Victorian Holocaust: El Niño Famines and the Making of the Third World* (Verso, London).
- 11 Cane MA, Zebiak SE, Dolan SC (1996) Experimental forecasts of El Niño. *Nature* 321(6073):827–832.
- 12 Latif M, et al. (1994) A review of ENSO prediction studies. *Clim Dyn* 9(4-5):167–179.
- 13 Tziperman E, Scher H (1997) Controlling spatiotemporal chaos in a realistic El Niño prediction model. *Phys Rev Lett* 79(6):1034–1037.
- 14 Kirtman BP, Schopf PS (1998) Decadal variability in ENSO predictability and prediction. *J Clim* 11(11):2804–2822.
- 15 Landsea CW, Knaff JA (2000) How much skill was there in forecasting the very strong 1997–98 El Niño? *Bull Am Meteorol Soc* 81(9):2107–2119.
- 16 Kirtman BP (2003) The COLA anomaly coupled model: Ensemble ENSO prediction. *Mon Weather Rev* 131(17):2324–2341.
- 17 Fedorov AV, Harper SL, Philander SG, Winter B, Wittenberg A (2003) How predictable is El Niño? *Bull Am Meteorol Soc* 84(7): 911–919.
- 18 Müller P, von Storch H (2004) *Computer Modelling in Atmospheric and Oceanic Sciences* (Springer, Berlin).
- 19 Chen D, Cane MA, Kaplan A, Zebiak SE, Huang D (2004) Predictability of El Niño over the past 148 years. *Nature* 428(6984): 733–736.
- 20 Palmer T, Hagedorn R (2006) *Predictability of Weather and Climate* (Cambridge Univ Press, Cambridge, UK).
- 21 Luo JJ, Masson S, Behera SK, Yamagata T (2008) Extended ENSO predictions using a fully coupled ocean-atmosphere model. *J Clim* 21(1):84–93.
- 22 Yeh SW, et al. (2009) El Niño in a changing climate. *Nature* 461(7263):511–514.
- 23 Chekroun MD, Kondrashov D, Ghil M (2011) Predicting stochastic systems by noise sampling, and application to the El Niño-Southern Oscillation. *Proc Natl Acad Sci USA* 108(29):11766–11771.
- 24 Galanti E, Tziperman E (2003) A study of ENSO prediction using a hybrid coupled model and the adjoint method for data assimilation. *Mon Weather Rev* 131(11):2748–2764.
- 25 Chen D, Cane MA (2008) El Niño prediction and predictability. *J Comput Phys* 227(7):3625–3640.
- 26 Penland C, Sardeshmukh PD (1995) The optimal growth of tropical sea surface temperature anomalies. *J Clim* 8(8):1999–2024.
- 27 International Research Institute for Climate and Society Earth Institute. IRI/CPC ENSO Quick Look. Available at <http://iri.columbia.edu/climate/ENSO/currentinfo/QuickLook.html>. Accessed November 30, 2012.
- 28 National Oceanic and Atmospheric Administration, National Centers for Environmental Prediction. Climate Prediction Center: ENSO Diagnostics Discussion. Available at http://www.cpc.ncep.noaa.gov/products/analysis_monitoring/enso_advisory/. Accessed November 30, 2012.
- 29 Webster PJ (1995) The annual cycle and the predictability of the tropical coupled ocean-atmosphere system. *Meteorol Atmos Phys* 56(1-2):33–55.
- 30 Goddard L, et al. (2001) Current approaches to seasonal to interannual climate predictions. *Int. J. Clim* 21(9):1111–1152.
- 31 Ludescher J, et al. (2013) Improved El Niño forecasting by cooperativity detection. *Proc Natl Acad Sci USA* 110(29): 11742–11745.
- 32 Donges JF, Zou Y, Marwan N, Kurths J (2009) The backbone of the climate network. *EPL. Europhys Lett* 87(4):48007.
- 33 Tsonis AA, Swanson KL, Roebber PJ (2006) What do networks have to do with climate? *Bull Am Meteorol Soc* 87(5):585–595.
- 34 Yamasaki K, Gozolchiani A, Havlin S (2008) Climate networks around the globe are significantly affected by El Niño. *Phys Rev Lett* 100(22):228501.
- 35 Gozolchiani A, Havlin S, Yamasaki K (2011) Emergence of El Niño as an autonomous component in the climate network. *Phys Rev Lett* 107(14):148501.
- 36 IPCC (2013) *Climate Change 2013: The Physical Science Basis. Contribution of Working Group I to the Fifth Assessment Report of the Intergovernmental Panel on Climate Change*, eds Stocker TF, et al. (Cambridge Univ Press, Cambridge, UK).
- 37 Foster G, Rahmstorf S (2011) Global temperature evolution 1979–2010. *Environ Res Lett* 6(4):044022.
- 38 Kosaka Y, Xie SP (2013) Recent global-warming hiatus tied to equatorial Pacific surface cooling. *Nature* 501(7467):403–407.
- 39 Li C, von Storch JS, Marotzke J (2013) Deep-ocean heat uptake and equilibrium climate response. *Clim Dyn* 40(5-6):1071–1086.
- 40 NASA GISS surface temperature analysis (GISTEMP). Available at <http://www.data.giss.nasa.gov/gistemp/>. Accessed November 30, 2012.
- 41 Kalnay E, et al. (1996) The NCEP/NCAR 40-year reanalysis project. *Bull Am Meteorol Soc* 77(3):437–471.
- 42 National Oceanic and Atmospheric Administration, Earth System Research Laboratory. NCEP/NCAR Reanalysis 1. Available at www.esrl.noaa.gov/psd/data/gridded/data.ncep.reanalysis.html. Accessed November 30, 2012.